Chapter: II

Synthesis of Various Half Doped Nanocrystalline Manganites by Combustion and Sol-Gel Method

Chapter-II

2.1 Introduction

During the last few decades, the nanocrystalline forms of various materials have attracted considerable attention because of the particle size dependent variations in the physical and chemical properties as we go down to the nanoscale, as compared to their bulk counterparts. Ceramics are no exceptions and particle size dependent properties have been investigated in many ceramic oxides. The solid state route, which is usually used to synthesize bulk ceramic powders need high sintering temperatures and longer time to obtain homogeneous composition, and is thus unsuitable for synthesizing nano-powders. Several techniques are in use today to synthesize nanocrystalline powders of ceramic oxides, such as sol-gel technique, hydrothermal synthesis and co-precipitation [Bell et al. (2000); Zhang et al. (2000); Chick et al. (1990)], spray drying, freeze drying, mechanical milling and so forth [Rahaman (1995)].

Among the various synthesis techniques, combustion synthesis is one of the most helpful chemical routes for synthesizing advanced materials in nanocrystalline forms [Merzhanov et al. (1972); Munir et al. (1989); Moore et al. (1995); Hlavacek et al. (1996); Varma et al. (1998); Mukasyan et al. (2005); Ravindranathanan et al. (1986); Chick et al. (1996)]. It offers several advantages [Mukasyan et al. (2007)] such as,

1. The initial reaction media being in the liquid state allows the mixing of the reactants on the atomic level.

2. High reaction temperature for very short duration ensures high product purity and crystallinity, and on optimizing the parameters, allow us to synthesize the powders without the step of calcination [Markovic et al. (2008)].

3. Short process duration and the formation of various gases during the combustion synthesis inhibits particle growth and favors the synthesis of nanopowders [Patil et al. (1997); Mukasyan et al. (2001); Patil et al. (2003); Varma et al. (2003); Deshpande et al. (2004)].

4. A comparative study [Conceicao et al. (2009)] of the effects of various synthesis techniques on the structure, particles size electrical and magnetic properties of manganites, showed that the combustion technique gave the smallest particle size and better homogeneity of the product.

2.2 Basic Process of Combustion Synthesis

The combustion synthesis consists in bringing a saturated aqueous acidic solution of the desired metal salts and a suitable organic fuel to boil, until the mixture ignites and a self sustaining and rather fast combustion reaction takes place, resulting in a dry, usually crystalline, fine powder. To produce a complex oxide, a mixture containing the desired metal ions in the form of say, water soluble nitrate salts and a fuel such as glycine or urea can be used [Patil et al. (2003a); Mukasyan et al. (2001); Patil et al. (2003b)]. While redox reactions such as this are exothermic in nature, and often lead to explosion if not controlled, the combustion of metal nitrates-glycine mixtures usually occurs as a self-propagating and nonexplosive exothermic reaction. The ignition of large amount of gases formed can result in the appearance of the flame, which can

reach temperatures in excess of 1000 ^{o}C for very short duration. The fuels used serve two purposes:

1. They are source of C and H which on combustion will form CO_2, H_2O and liberate heat.
2. They form complexes with the metal ions facilitating homogeneous mixing of the cations in solution.

By simple calcinations, the metal nitrates can, of course, be decomposed into metal oxides upon heating to or above the required temperature. A constant external heat supply is necessary in this case, to maintain the system at the high temperature required, accomplishing the appropriate phase transition or decomposition. In combustion synthesis, the energy released from the exothermic reaction between the nitrates and the fuel, which is usually ignited at a temperature, can rapidly heat the system to a high temperature and sustain it long enough, even in the absence of a heat source, for the synthesis to occur.

2.3 Basic Principles of Calculations

The concept of the combustion synthesis techniques comes from the thermo chemical concepts used in the field of propellants and explosives. Jain et al. (1981) devised a simple method of calculating the oxidizing to reducing character of the mixture, which consists of establishing a simple valency balance, irrespective of whether the elements are present in the oxidizer or the fuel components of the mixture, to calculate the stoichiometric composition of the redox mixture which corresponds to the release of the maximum energy for the reaction. The assumed valencies are those

presented by the elements in the usual products of the combustion reactions, which are CO_2, H_2O and N_2. Therefore, the elements C and H are considered as reducing elements with the corresponding valencies +4 and +1, oxygen is considered an oxidizing element with the valency -2 and nitrogen is considered with zero valency. In combustion reaction, as oxidizers, metal nitrates are preferred, since they are water soluble, and a few hundred degrees is sufficient for their decomposition. The total valency in many divalent nitrates is -10 and in trivalent nitrates is -15. Also, it has been shown [Fumo et al. (1996)] that the most favored products of combustion synthesis carried out with nitrates are indeed N_2 and O_2.

Once we calculate the amounts of the nitrates salts and the glycine to be used in the process, we can write down the various chemical reactions that might be involved in the process, and calculate the enthalpy of the reaction [Sibey et al. (2000)], using this relation.

$$\Delta H^\circ = (\Sigma\ n.\ \Delta H_f^\circ)_{products} - (\Sigma\ n.\ \Delta H_f^\circ)_{reactants}$$

where n is the number of moles and ΔH° is the enthalpy.

This can be calculated in terms of 'x' which is the number of moles of glycine in the system. Then, the following equation can be used to theoretically approximate the adiabatic flame temperature for the combustion synthesis [Selvan et al. (2009)].

$$Q = -\Delta H^\circ = \int_{298}^{T} (\Sigma\ n.\ cp)\,products\ dT$$

where Q is the heat absorbed by the products under adiabatic conditions, and c_p is the heat capacity of the products at constant pressure.

Besides glycine, various other fuels have been used such as urea, maleic anhydride, carbohydrazide etc. All of these fuels contain nitrogen, but differ in their “reducing power” and the amount of gases they generate, which affects the characteristics of the reaction product. Larger amount of gases dissipate more heat, thereby preventing the oxides from calcinations since the temperature reached is not so high, and so, nanoparticles may not be formed. On the other hand, a low amount of fuel, might affect the flame temperature reached, thereby causing incomplete decomposition in the reaction mixture and formation of other phases in the final product.

Thus, the various parameters to be considered in combustion synthesis method are pH, Fuel/oxidizer ratio, nature of fuel etc. Several studies have been performed on the effects of these parameters on the final product [Deganello et al. (2009)], and in particular on the effect of the propellant [Conceicao et al. (2009)].

2.4 Characterization Tools

2.4.1 X-ray Diffraction

X-ray diffraction technique is a powerful tool used to characterize and x-ray refine the structure and different phases present in any material. Powder diffraction patterns are the characteristic of given materials and each material produces its own diffraction pattern which is distinct from any other material. The great advantage of powder x-ray diffraction technique is also found in the chemical analysis, stress measurement, study of phase equilibrium, determination of particle size and in-situ measurements. In the present work, the calcined and sintered powders were characterized for structure and phase analysis using powder x-ray diffraction measurements. X-ray diffraction (XRD)

measurements were carried out using an 18kW rotating anode (CuKα) based Rigaku (Japan) powder diffractometer operating in the Bragg-Brentano geometry and fitted with a graphite monochromator in the diffracted beam.

2.4.2 Scanning Electron Microscopy

It is an important non-destructive tool to analyze the magnified images of metallic, semiconducting and insulating materials. It uses accelerated electrons instead of visible light to form an image. A stream of electrons is produced by an electron gun and is accelerated from few hundred eV to 40 keV. The electron beam follows a vertical path through the microscope, which is held in within a high vacuum. The beam is focused using magnetic lenses to a spot size of about 0.4 to 5 nm in diameter on the sample surface. Once the beam hits the sample, electrons and x-rays are ejected from it. Detectors collect these x-rays, backscattered electrons, secondary electrons and convert them into an image/signal that can be visualized on a computer screen. The electron beam is scanned, or 'rastered' across the sample via magnetic scan coils. The current produced due to the backscattered electrons is collected, amplified and plotted as a two-dimensional 'micrograph' image of the signal intensity. For SEM, samples should be conducting to ensure no charging during the measurement. The samples were mounted on the sample holder using carbon tapes.

For the present study, a field emission gun based scanning electron microscope (FE-SEM) (Supra 40, Zeiss, Germany), equipped with energy dispersive x-ray analyzer was used. The half doped $R_{0.5}A_{0.5}MnO_3$ (R = La, Nd, Sm and A = Ca, Sr) nanoparticles were coated with conducting gold layer by sputtering under vacuum before recording

the images to avoid charging. The gun voltage was varied to capture well focused image of the sample. Compositional analysis was carried out by the energy dispersive x-ray spectroscopy (EDS) available with the above system. Its working principle is that each element has a unique atomic structure allowing emission of x-rays that are characteristic of that particular element which is distinguishable from the x-rays emitted by another element.

2.4.3 Transmission Electron Microscopy

Transmission electron microscopy (TEM) uses high energy electrons to penetrate through a thin (≤ 100 nm) sample. This offers increased spatial resolution in imaging (down to atomic scales) as well as the possibility of carrying out diffraction from nano-sized volumes. When electrons are accelerated upto high energy levels (few hundreds keV) and focused on a material, they can scatter or backscatter elastically or in elastically, or produce many interactions, source of different signals such as x-rays, Auger electrons or light [Willams and Carter (1996)]. To find out the size, shape of half doped $R_{0.5}A_{0.5}MnO_3$ (R = La, Nd, Sm and A = Ca, Sr) nanoparticles, we used a TEM from Tecnai G2T 30. For sample preparation of the powder samples, few milligram of the powder was dispersed in 50 ml of ethanol and ultrasonicated for homogeneous mixing. Then a drop from the solution was casted on the commercial TEM grids (carbon coated copper grids). Further, the grid was dried to evaporate the volatile alcohol. Similar method was adopted for investigating $R_{0.5}A_{0.5}MnO_3$ (R = La, Nd, Sm and A = Ca, Sr) samples.

2.4.4 Magnetic Measurements

Magnetic measurements reveal the magnetic state of a material. The basic measurements include the measurement of magnetization as a function of temperature with a constant probing field. Magnetization as a function of applied external magnetic field at constant temperature also helps to get the magnetic behaviour of the material. In this work for magnetic characterizations, we used a commercial VSM (PPMS from Quantum Design, USA), a superconducting quantum interference device (SQUID: MPMS XL from Quantum Design, USA) and superconducting quantum interference device - vibrating sample magnetometer (SQUID-VSM from Quantum Design, USA). The facilities were utilized at UGC-DAE CSR, Indore, India. Brief descriptions of the working principle of each are given below.

2.4.4.1 Vibrating Sample Magnetometer (VSM)

DC magnetization measurements of half doped $R_{0.5}A_{0.5}MnO_3$ (R = La, Nd, Sm and A = Ca, Sr) nanoparticles were carried out using a commercial VSM having specification with temperature variation from 2 - 400 K and magnetic field ± 14 Tesla. For the measurement of magnetic moment, a VSM involves induction method that refers to the measurement of voltage induced in a set of detection coils by a varying magnetic moment. In this process, sample under investigation is vibrated in a uniform magnetic field, which induces voltage at the detection coil. For instance, if a magnetic dipole, initially placed in the center of a pickup (detection) coil, is moved to a distance then a flux (Φ) is produced which results in inducing a voltage ($v = d\,\Phi/dt$) in the detection coil. The pickup coils may be located inside a solenoid (for generating

magnetic field), so that the moment can be measured as a function of the externally applied magnetic field [Foner (1959)].

2.4.4.2 SQUID Magnetometer

Superconducting Quantum Interference Device (SQUID) is the most sensitive instrument available to measure the magnetic field. However, it does not detect the magnetic field from the sample directly. The sample is made to move through superconducting detection coils, which are coupled to the SQUID through superconducting wires, allowing the current from the detection coils to inductively couple to the SQUID sensor. The basic function of a SQUID is to convert current to voltage sensibly. The instrument essentially contains the following parts: the SQUID (main unit of the device), a magnetic flux transformer including pickup coils, the superconducting magnetic coil, heat switches and magnetic shielding. Superconducting detection coils are configured as a second-order gradiometer, with counter wound outer loops which make the set of coils non-responsive to uniform magnetic fields and linear magnetic field gradients. The detection coils only generate a current in response to local magnetic field disturbances [Clarke (1996)]. The superconducting magnetic coils are used to apply large magnetic fields. Since SQUID is extremely sensitive to minute fluctuations of the magnetic field, magnetic shielding is inevitable to shield the sensor itself both from the fluctuations in the ambient magnetic field of the laboratory and from the large magnetic fields produced by the superconducting coil. Heaters are used to heat up a small section of the detection coil circuit whenever the magnetic field is

changed. They allow the elimination of standing currents in the superconducting loops by heating them beyond their critical temperature.

2.4.4.3 SQUID–Vibrating Sample Magnetometer (SQUID-VSM)

It is a modified version of SQUID magnetometer. It records the magnetic moment of the sample combining the sensitivity of a SQUID and speed of a VSM. The sample is vibrated at a known frequency and phase-sensitive detection is employed for rapid data collection and spurious signal rejection. It is worth noting here that the sample vibration is anyhow not the essential requirement to produce the signal as in a conventional copper-detection-coil VSM where a changing magnetic flux is a must. Instead, the sample vibration is used only to create a signal at a known modulation frequency to aid the separation of the sample signals from the instrumental artifacts. The size of the signal does not depend on the vibration frequency and higher vibration frequencies will not improve the signal to noise ratio, as in a conventional VSM. This is due to the use of superconducting detection coils which produces a current in response to magnetic flux, rather than to a change in magnetic flux as produced by copper coils.

2.4.5 X-ray Photoelectron Spectroscopy (XPS)

X-ray photoemission spectroscopy (XPS) or “electron spectroscopy for chemical analysis (ESCA)” is a surface sensitive technique that provides information about the chemical composition (atomic percent of elements present in the sample), oxidation state (chemical state) of the constituent elements and valance band structure (density of occupied electronic states). XPS is based on the principle of photoelectric effect. When

the sample is exposed to mono energetic x-ray photons of energy hν, it emits electrons from the sample surface. The emitted electrons have kinetic energy (K.E.) given by

$$K.E. = h\nu - B.E. - \Phi$$

Where "hν" is the energy of the incident photon, "B.E." is the binding energy of the electron and "Φ"is the work function. From the above equation, it is clear that photoelectrons can be produced only if $h\nu \geq B.E. + \Phi$ [Stickle (1992)]. The emitted electrons are sorted by their K.E. and the spectrum obtained is a plot of number of emitted electrons per energy interval versus their K.E., known as energy distribution curve (EDC). Since the energy hν of the exciting photons is kept fixed, the B.E. of the electronic states relative to Fermi energy level (EF) can be determined by measuring the K.E. distribution of the photoelectrons. Therefore, the energy distribution of the photoelectrons corresponds approximately to the energy distribution of electronic states in the solid. The photoexcited electrons may scatter with other electrons, plasmons, phonons, and consequently loose part of their energy so that it may not have enough energy to be able to escape at all and change their momentum. One of the consequences of such scattering is the secondary inelastic background intensity, which becomes dominant at the low K.E., principally due to the electron-electron scattering. Since on an average, a photo electron can travel over a mean free path before being scattered, the electron from a depth of few Å only can reach the detector, making it a surface sensitive technique in spite of large penetration power of X-rays. Finally, the escape from the solid is possible only for those electrons with a K.E. component normal to the surface that is sufficient to surmount the potential barrier offered by its work function. For photoelectron spectroscopy, three main components are required: (i)

a photon source, (ii) an energy analyzer for photoelectrons, and (iii) an electron detector. High vacuum is needed to increase the mean free path of the electrons coming out of the sample surface and reaching the detector, and to reduce the contamination layer covering over the sample surface during measurement. Since the photoelectron energy depends on the source energy, the excitation source must by monochromatic. The energy of the photoelectrons is analyzed by an electrostatic analyzer.

In the present study, we employed XPS instruments from VSW and AMICUS using Al-Kα (1486.6 eV) and Mg-Kα (1253.6 eV) radiations, respectively. The vacuum level of the sample preparation chamber (SPC) was ~ 10-8 Torr and the sample analysis chamber (SAC) was ~ 10-9 Torr. First, we scanned over the full energy range (survey scan), and then specifically selected Mn 2p core level spectra for our study. All observed peaks were calibrated to C 1s peak at 284.8 eV. XPS data were fitted using XPSPEAK4.1 software package.

2.5 Samples Preparation

2.5.1 By Chemical Combustion Technique

Samples used in the present work were prepared by chemical combustion synthesis route. $La_2O_3.H_2O$ (Himedia ~99.9%), Pr_6O_{11} (Himedia ~99.0%), Nd_2O_3 (Himedia ~99.0%), Sm_2O_3 (Himedia ~99.0%), $SrCO_3$ (Himedia ~99.0%) and $CaCO_3$ (Himedia ~99.0%) were used as reactants. The oxides were first converted into nitrates by dissolving them into dilute nitric acid. The $Mn(CH_3COO)_2.4H_2O$ (Qualigens ~99.0%) was dissolved in distilled water. The reactant solutions were mixed in a beaker and water solution of glycine ($C_2H_5NO_2$) (99.7%) used as fuel, was then added.

The resulting solution was kept at hot plate with continuous stirring. With the evaporation of solvent the solution thickened with blackish colour and eventually ignited after some time. After combustion dark brown powder was obtained. This powder was divided into several parts which were calcined at various temperatures for 6 hours to get samples of various particle sizes. Figure 2.1 shows the flow chart for the process. Using this method, samples of half doped $R_{0.5}A_{0.5}MnO_3$ (R=La, Sm, Nd, Pr and A=Ca, Sr etc) nanocrystalline manganites were synthesized.

The XRD patterns of $R_{0.5}A_{0.5}MnO_3$ (R=La, Sm, Nd, Pr and A=Ca, Sr etc) calcined at various temperatures 600, 700, 800, 900, 1000, 1100, 1200, 1300 and 1400 ^oC are shown in Fig. 2.2 to Fig. 2.7. All the peaks in the XRD patterns of the calcined powders shown in Fig. 2.2 to Fig. 2.7 could be indexed with the pure perovskite structure. The crystallite/particle were calculated using Scherrer formula, given bellow.

$$t = \frac{0.9\lambda}{B\cos\theta}$$

where B is usually measured width (angular width) of the peak in term of 2θ in radians, λ is wave length of x-ray diffraction, using this formula, we have found crystallite/particle size of the calcined powder are the range of 20 nm to few 100 nm for nano samples.

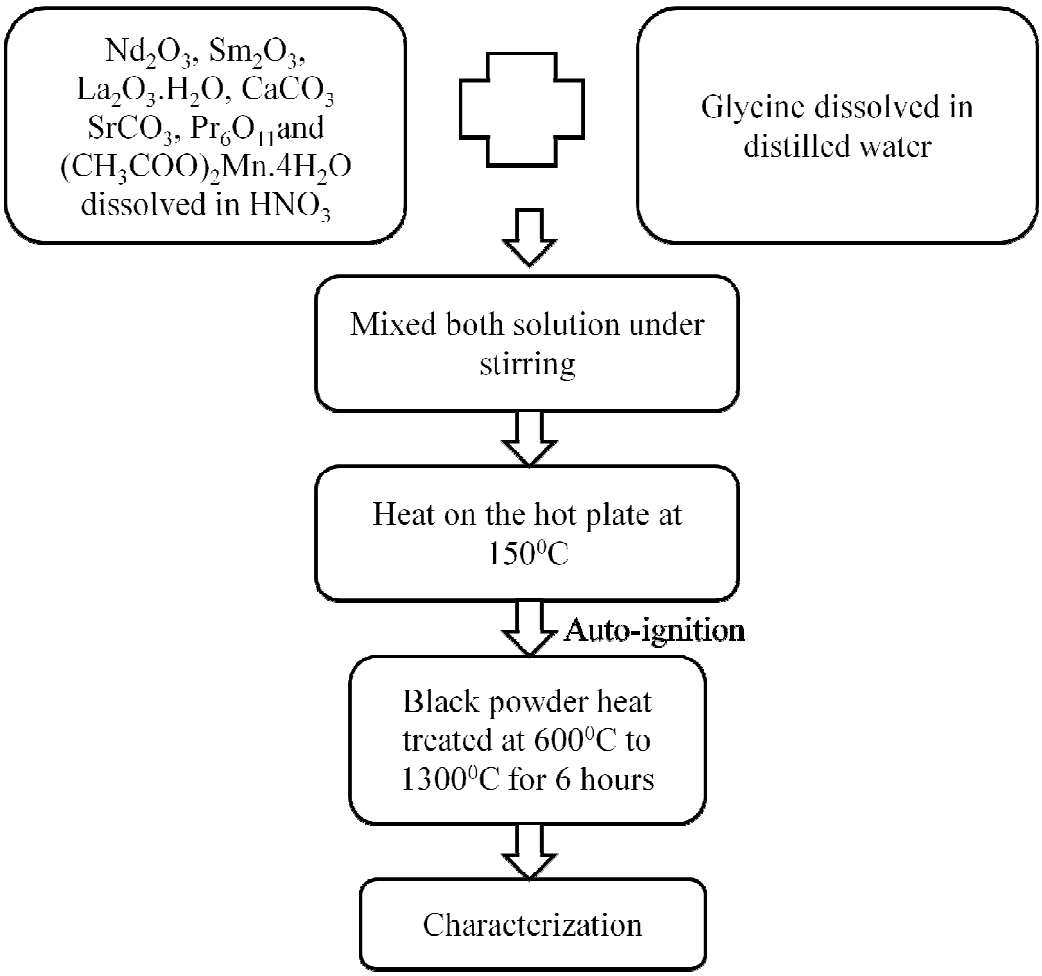

Fig. 2.1 Flow chart depicting combustion synthesis.

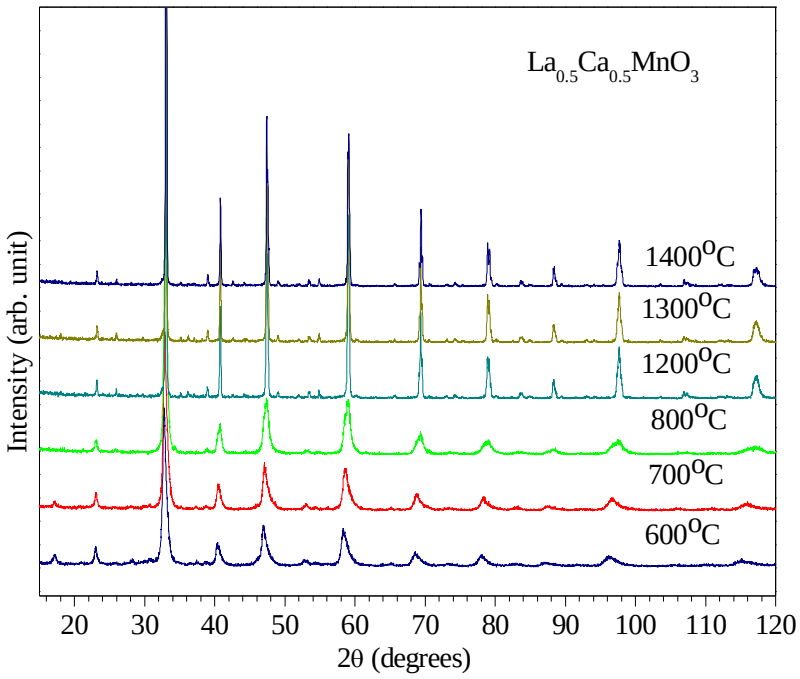

Fig. 2.2. Room temperature XRD patterns of $La_{0.5}Ca_{0.5}MnO_3$ nanoparticles prepared at various calcination temperatures.

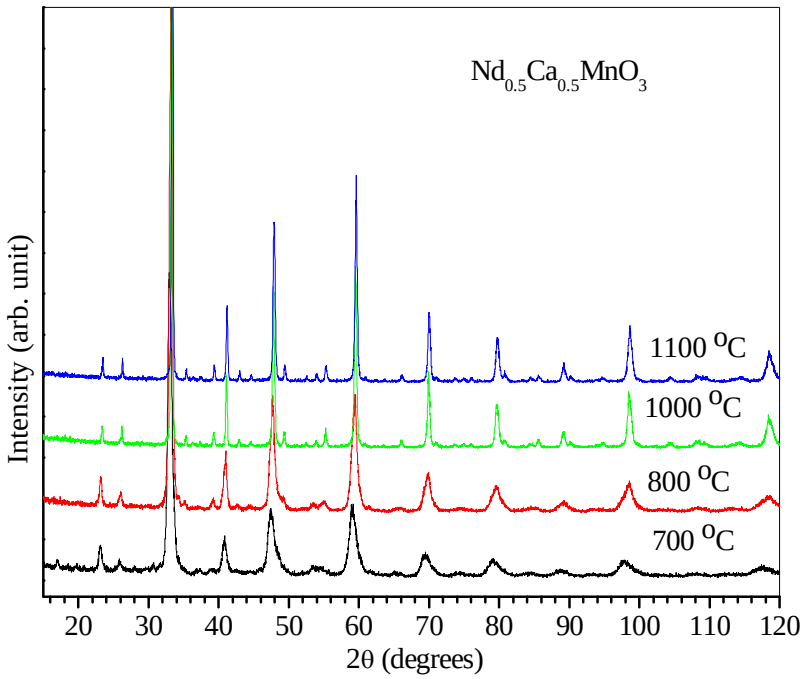

Fig. 2.3. Room temperature XRD patterns of $Nd_{0.5}Ca_{0.5}MnO_3$ nanoparticles prepared at various calcination temperatures.

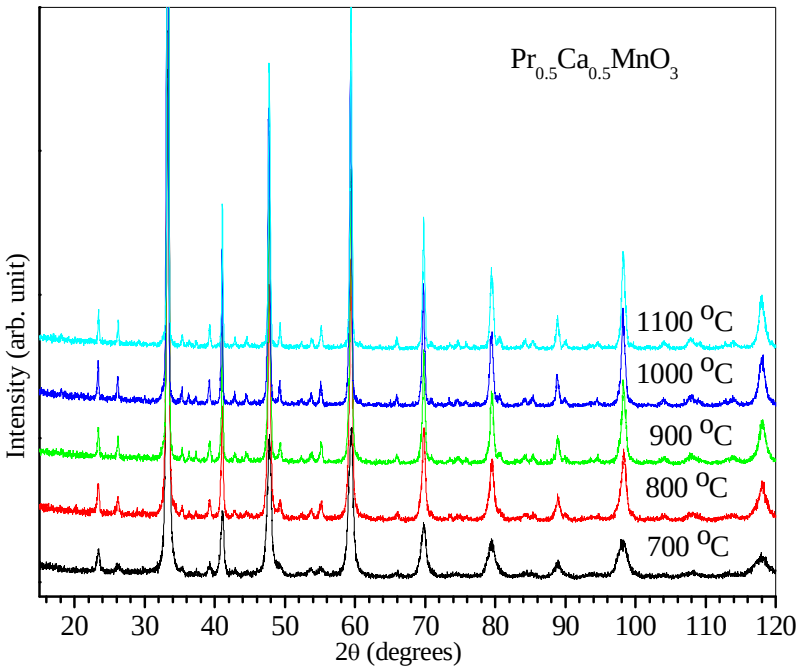

Fig. 2.4. Room temperature XRD patterns for $Pr_{0.5}Ca_{0.5}MnO_3$ nanoparticles prepared at various calcination temperatures.

.

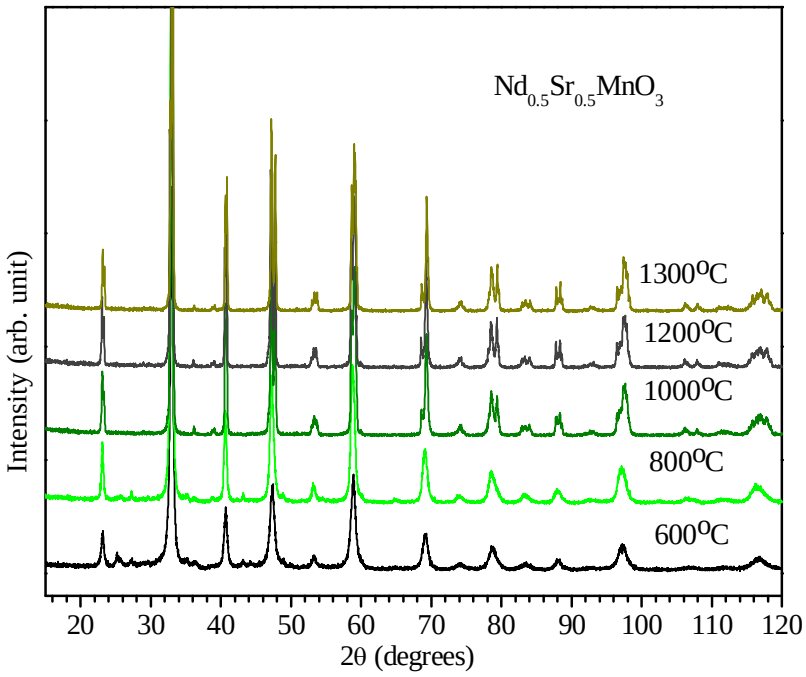

Fig. 2.5. Room temperature XRD patterns for $Nd_{0.5}Sr_{0.5}MnO_3$ nanoparticles prepared at various calcination temperatures.

.

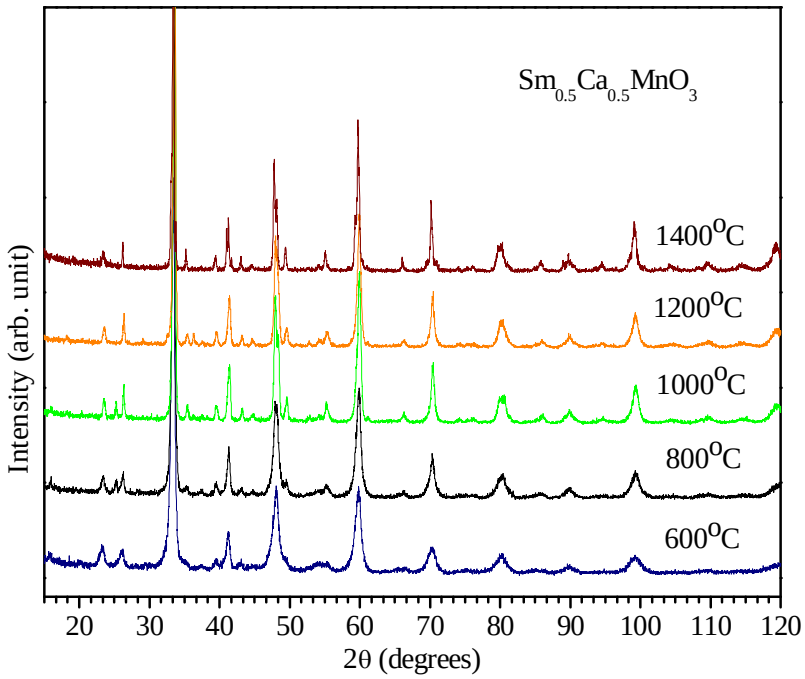

Fig. 2.6. Room temperature XRD patterns for $Sm_{0.5}Ca_{0.5}MnO_3$ nanoparticles prepared at various calcination temperatures.

2.5.2 Synthesis of $La_{0.5}Ca_{0.5}MnO_3$ by Chemical Sol-Gel technique

The history of sol-gel processing began in the mid-1800s with Ebelman and Graham's studies on silica gels [Larry et al. (1990)]. Sols are dispersions of colloidal particles in liquid. Colloids are solid particles with diameters of 1-100 nm. A gel is a interconnected, rigid network with pores of sub-micrometer dimensions and polymeric chains whose average length is greater than a micrometer [Larry et al. (1990)]. However the sol-gel process has potential advantage over the other methods not only for achieving homogeneous mixing of the components on the atomic scale but also for possibility of forming desired morphologies which are of the technological importance. In sol-gel process, 'sol' is a suspension of colloidal particles in a liquid or a solution of polymer. 'Gel' is the semi rigid mass formed when the colloidal particles are linked by the surface forces to form a network or when the polymer molecules are cross linked. In sol-gel process, a solution of metal compounds or a suspension of very fine particles in a liquid (sol) is converted into a semi-rigid mass (gel). We prepared the solution of $La_2O_3.H_2O$, and $CaCO_3$ by dissolving in conc. HNO_3 acid and $Mn(CH_3COO)_2.4H_2O$ in distilled water , maintaining stoichiometric proportion needed for $La_{0.5}Ca_{0.5}MnO_3$. An equal amount of ethylene glycol was added to this solution with continuous stirring. This solution was then heated on a hot plate at a temperature of ~140 ºC till a dry thick brown color gel is formed. At this temperature ethylene glycol polymerizes into polyethylene glycol, which disperse the cations homogeneously forming a cation polymer network. This had been further decomposed in an oven at a temperature of ~300 ºC to get a polymeric precursor in the form of black resin material. The polymeric

precursor was heat treated at several temperatures viz. 550, 600, 700, 800, 900, 1000, 1100, 1200 and 1300 ºC for a time period of 4 hours to get LCMO samples of different particles sizes.

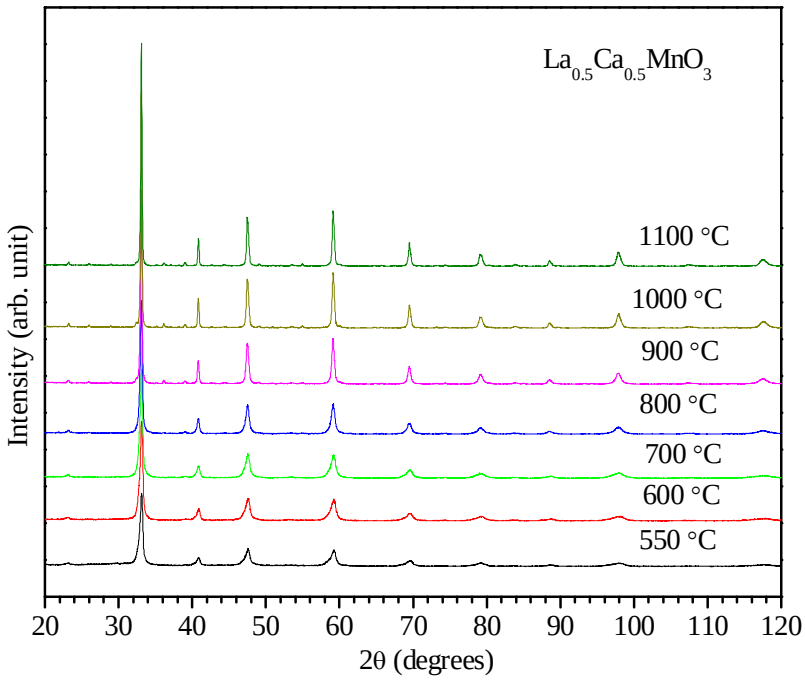

Fig. 2.7. Room temperature XRD patterns of $La_{0.5}Ca_{0.5}MnO_3$ nanoparticles prepared at various calcination temperatures using Sol-Gel method.

2.6 Summary

Pure perovskite phase samples of half doped $R_{0.5}A_{0.5}MnO_3$ (R = La, Nd, Sm and A = Ca, Sr) nanoparticles were synthesized under optimized conditions by using combustion synthesis method. The $La_{0.5}Ca_{0.5}MnO_3$ was synthesized by sol-gel method also. Powders of same batch were calcined at various temperature to get samples of various crystallite sizes from nano to bulk. The crystallite size of the nano samples was obtained in the range of ~20 nm to few 100 nm for different calcination temperatures.